

# Analytical Study of Hip Sliding Mechanisms in Seating Using Human FE Model

Authors

Shigeki Hayashi<sup>1)</sup>, Tsuyoshi Yasuki<sup>1)</sup>, Yuichi Kitagawa<sup>1)</sup>, Yoshiki Takahira<sup>2)</sup>

1) Toyota Motor Corporation, Toyota, Japan

2) Toyota Technical Development Corporation, Toyota, Japan

## Summary:

This paper describes hip sliding mechanisms for seating comfort evaluation using a human FE model (THUMS). From a rigid seat experiment, combined with THUMS simulation, it was first found that the backward moment around the hip centre of gravity induced by the hip seat reaction force on pelvis was the main cause of hip sliding. A hip sliding equation was then constructed considering seat characteristics, namely hip seat cushion angle and hip seat reaction force, as parameters. Finally, a validation of this equation was conducted asking test subjects to seat in prototype automotive seats.

## Keywords:

Seat, Comfort, Human FE Model, Hip Sliding

## 1 Introduction

Seating comfort is one of the important performances in automotives. Hip sliding is the phenomenon occurring when occupant's pelvis moves forwards gradually during seating. It induces a change in seating posture and affects seating comfort. It is said that hip sliding induces change of seating posture and affects the seating comfort performances. Hip sliding is often evaluated subjectively and requires tests with several volunteers. An objective evaluation, which could link subjects' feeling and physical measurements, would help to set-up design requirements. Matsuoka et al. [1] reported a condition of hip sliding for railway seat using mass spring human model. In this technique, weight distribution of the human body to the mass model affects the accuracy of the sliding results. A similar evaluation using finite element model, which represents accurately human body shape and mass distribution, has been recently proposed by Hwang et al. [2]. They developed a human FE model based on measurement of volunteer's hip shape, muscles and skin thickness. Using the developed model, they simulated seating conditions and reproduced the pressure distribution between the body and the seat skin. Rammussen et al. [3] developed a human model including principal muscles (Anybody TM) and evaluated the effect of backrest angle on muscle forces and seating shear force generated between the human model and the seat.

In this study, mechanisms of hip sliding generated in automotive seat are studied using a human FE model which has the ability to simulate seating condition precisely. The study focused on displacement of the pressure distribution underneath the ischium tuberosities. A quantitative evaluation of hip sliding was derived from those results. A hip sliding equation was constructed based on the relationship between the seat cushion angle underneath the hip and the interaction force by relating it to the moment around the hip centre of gravity. Moreover, the hip sliding equation was verified by sensory evaluation of prototype seats referring to the equation.

## 2 Methodology

### 2.1 Development of human FE model

This study used the Total Human Model for Safety (THUMS) developed in collaboration with Toyota Motor corporation and Toyota Central R&D Labs, Inc.. THUMS represents an average sized American adult male person with a height of 175 cm and weighing 77kg (AM50). The THUMS shown in Figure 1 includes major components in the human body, such as bones, internal organs, and ligaments connecting bones. Joints are modeled by contact between bones. The LS-DYNA™ code commonly used for FE analysis was used for this study. Characteristics of muscles around the hip considered to affect hip sliding were reviewed. The initial compression property of the hip flesh was referred from Yamada et al. [4]. The initial posture of the pelvis and lumbar vertebra greatly influences the hip sliding. The pelvis posture of the model was derived from X-rays of a driver [5]. THUMS pelvis angle was adjusted to match subject's one measured on X-rays and defined as the line passing through the middle of both ischium tuberosities and upper portion of sacrum (Figure 2).



Fig. 1: Human FE Model THUMS(AM50)

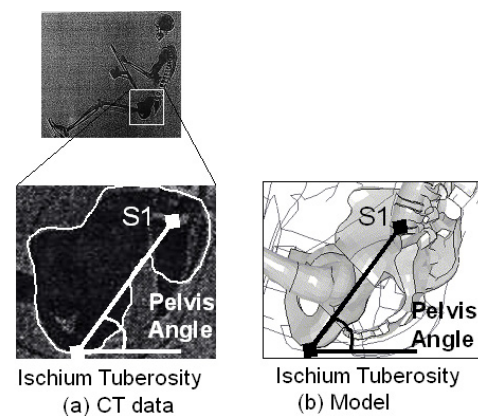


Fig. 2: Pelvis Posture

## 2.2 Evaluation of Hip Sliding

Hip sliding is caused by a pelvis rotation that induces a forward movement of the ischium tuberosities. In this study, it is assumed that reaction force from the seat induces the pelvis rotation. Therefore this study attempts to clarify the mechanisms of the hip sliding considering the moment around the hip's centre of gravity.

The location of the seat reaction force was studied on a flat rigid seat. The seat was divided and a hinge mechanism was installed at 135 mm from the rear end to adjust thigh angle. The rear part of the seat (underneath the hip, called „hip seat angle“) and its front part (underneath the thighs, called „thigh seat angle“) could be adjusted independently: from 0 to 20 degrees for the rear part and from 0 to 25 degree for the front part. The backrest angle was fixed at 21 degrees in all cases. An experiment was conducted with a subject (176 cm height, 74kg weight) whose anthropometry is close to AM50. A sensor mat was set on the seat and the backrest to measure the pressure distribution. The sensor mat consisted of 43 X 49 sensors (10 X 10 mm pitch) and the sensing area was 420 X 480 mm. In general, highest pressure points were recorded at the ischium tuberosities. The amount of hip sliding was defined by the displacement of these two pressure points. In order to minimize the effect of friction between clothes and skin, and the muscular effort to maintain the posture, the sensor mat was wrapped in plastic film and the subject was requested to take a relax posture. The subject was asked whether he could feel his hip sliding. For comparison with FE model, anatomical landmarks were measured on the subject using a 3D arm system: on head (ears), 7<sup>th</sup> cervical spine vertebra, greater trochanters, knees and ankles.

In simulation, THUMS was seated on a flat rigid seat and gravity was applied to it (Figure 3). The posture of the THUMS was steady after 1 second simulation time. THUMS anthropometry (175 cm height and 77 kg weight) was similar to subject's one (176 cm height and 74 kg weight). The 1 cm difference in total height was found to be due to a difference in THUMS and the subject torso length (from head to femoral trochanter via neck). It is expected that this 1 cm difference does not affect so much the hip sliding magnitude. The amount of hip sliding in the FE analysis was defined as the displacement of ischium tuberosities before and after seating.

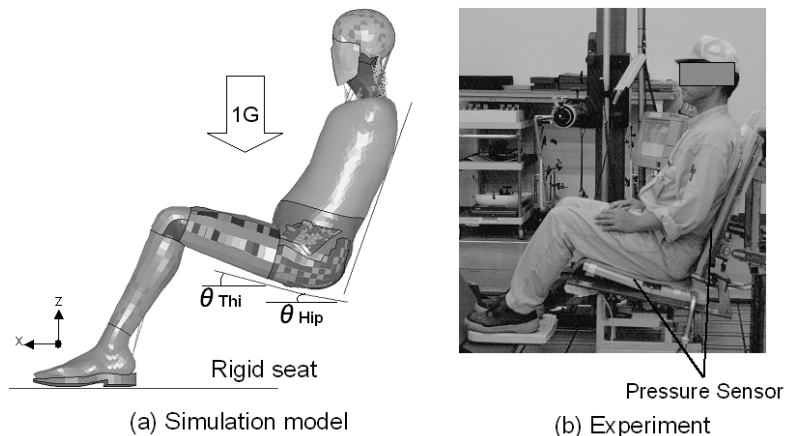


Fig. 3: Hip Sliding Evaluation on Rigid Seat

## 3 Hip Sliding Mechanisms and Equation

### 3.1 Experimental Result of Hip Sliding

Figure 4 shows the subjective evaluation results for different hip and thigh seat angles of the seat. A black mark is used when the subject indicated that he felt the hip sliding, and a white mark is used when he could not feel it. When the thigh seat angle was increased from 0 to 20 degrees, the subject did not feel the pelvis sliding until a hip seat angle of 13 degrees was reached. Moreover, hip sliding was not perceived by the subject when the hip angle was set at 10 degrees and the thigh seat angle was set until 24 degrees. The perception area was below the dotted line as shown in Figure 4. It is observed that the hip seat angle affects more the hip sliding perception than the thigh seat angle. The pressure distribution showed that the subject started to feel his hip motion for ischium tuberosities displacement from 6 mm (6 to 12 mm was measured in tests where the subject indicated his pelvis was moving). In the cases for which the subject did not announce that he felt a hip motion, only about

2 mm of tuberosities displacement was measured. These results show that the subject could sense 6 mm move forward of ischium tuberosities as hip sliding.

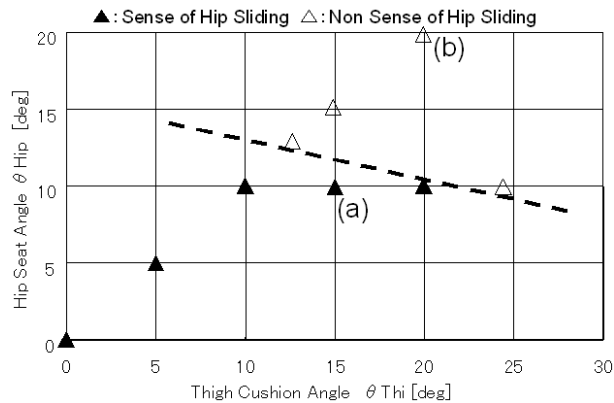


Fig. 4: Experimental Result of Hip Sliding Sense

### 3.2 Mechanism of Hip Sliding

The FE analysis using THUMS was conducted in one case of hip sliding (case (a) in Figure 4) and in the case of non hip sliding (case (b) in Figure 4). The simulation results of the ischium tuberosities movement were 11 mm in the case hip sliding and 5 mm in the case of non hip sliding respectively. These simulation results agree with the experimental results. Figure 5 shows applied force vector to the hip in the sliding case (a) and in the non sliding case (b). The force from the hip seat part to ischium tuberosities is larger than other forces to the hip, such as from femur, abdomen, spine, and backrest. The hip force, represented by a thick vector in the figure 5, equals 470 N and 446 N in the hip sliding case and non hip sliding case respectively. The reason of the relatively smaller hip force in non hip sliding case (b) is the thigh seat angle set to 20 degrees, compared to 15 degrees in sliding case (a), which causes some forces to be distributed to thigh area. The hip vector in the case of hip sliding case (a) has more offset from the centre of gravity of hip comparing to the non hip sliding case (b). As expected, this offset of vector from the hip centre of gravity generates the moment to rotate the hip in clockwise direction. The friction force between the hip and the hip seat was larger in sliding case (47 N) than in non hip sliding case (8 N). The rotation of the hip was limited by this friction force between hip and hip seat in the hip sliding case (a). Therefore, a study of moment balance around hip center of gravity allows to calculate the hip sliding factors. The moment around the hip centre of gravity was investigated for both hip sliding case (a) and non hip sliding case (b).

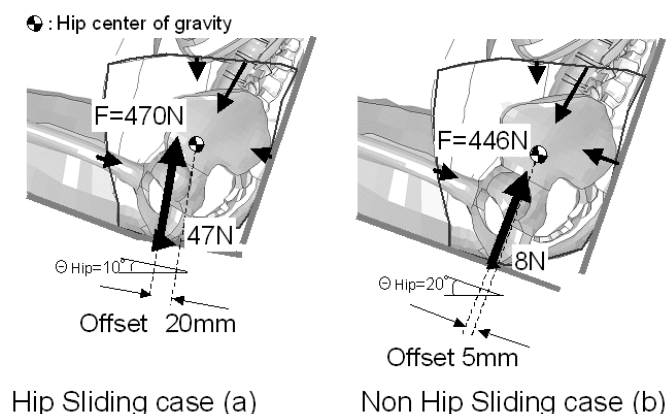


Fig. 5: Comparison of Applied Force to Hip

The moments of each force that is applied to the hip from seat (cushion, backrest), and human body (spine, abdomen, thighs) are shown in Figure 6. The positive moments in the figure generate the hip sliding, while the negative moments constrain hip rotation forward. From the results in case of hip sliding (a), it becomes clear that hip seat reaction force provides the larger contribution (9.4 Nm) to the

hip rotation, limited mostly by the friction between hip and seat (-5.6 Nm) and thigh force (-2.5 Nm). On the other hand, in the case non hip sliding (b), the moment of the hip seat was relatively lower (2.2 Nm) than that of hip sliding case, as the result, the moment magnitude created by the friction force was lower. It is then clear that the main cause of hip sliding is the hip seat reaction force and the more force or the more offset of the vector from the hip centre of gravity generates the more moment which induces the hip forward rotation.

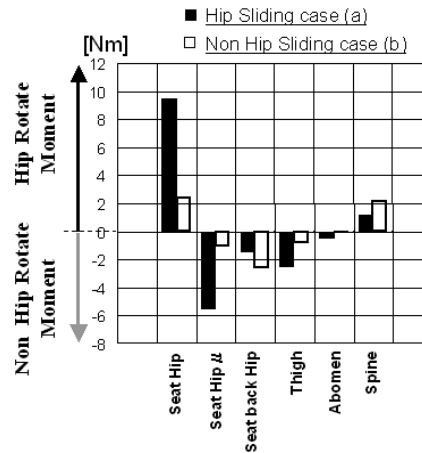


Fig. 6: Rotation Moment Balance of Hip

### 3.3 Hip Sliding Equation

Hip sliding equation based on the idea described in the previous session was derived in the relation between hip force and hip seat angle. The moment around hip centre of gravity is shown in Figure 7, and the balance is expressed as follows.

$$F_1 \times L_1 + F_6 \times L_6 - (F_2 \times L_2 + F_3 \times L_3 + F_4 \times L_4 + F_5 \times L_5) = 0 \quad (1)$$

Here,  $F_1$  shows the force underneath the hip (at tuberosities).  $L_1$  shows the distance from the  $F_1$  vector to the hip centre of gravity.  $F_2$  is the friction force between the hip and seat.  $L_2$  is the offset distance from the  $F_2$  vector to the hip centre of gravity. In the same manner,  $F_3$  and  $L_3$  are the force and offset distance from seat backrest,  $F_4$  and  $L_4$  are from thigh,  $F_5$  and  $L_5$  are from abdomen,  $F_6$  and  $L_6$  are from spine. From equation (1), after considering simple geometrical relations, an expression for limit  $F_1$  as a function of other forces and hip seat angle  $\theta_{Hip}$  can be obtained.

$$F_1 = \frac{F_2 \times L_2 - (F_3 \times L_3 + F_4 \times L_4 + F_5 \times L_5 + F_6 \times L_6)}{(L_p - H_p \times \tan \theta_{Hip}) \times \cos \theta_{Hip}} \quad (2)$$

Here,  $L_p$  and  $H_p$  are the distances, horizontal and vertical respectively, from the ischium tuberosities and the hip centre of gravity.

Hip sliding condition "equation (2)" is summarized in Figure 8 for the hip force range 300 N to 600 N, which is typical for seating application. The curve line in the figure corresponds to the equation (2). The area above the line contains non sliding seat conditions, and the area below the contrary. The graph shows the weak effect of hip force on sliding compared to hip seat angle. The circle marks are the experimental results.

Black circle marks are the hip sliding cases. And white circle marks are the non sliding cases. The hip force is calculated by cumulating the pressure map values under the hip area. The hip sliding cases are placed in the upper area of the equation line, and the non sliding cases are in the lower area of the line. It is confirmed that the equation (2) is applicable to estimate the generation of hip sliding.

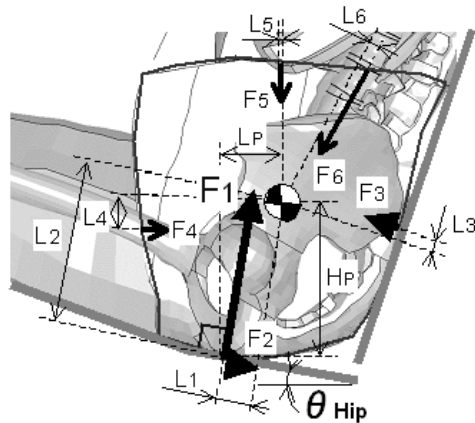


Fig. 7: Calculation of Moment of Hip

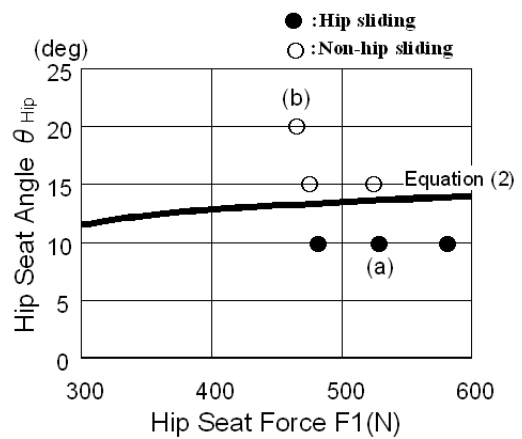


Fig. 8: Hip Sliding Condition

## 4 Estimation of Hip Sliding in Automotive Seat

### 4.1 Modeling of Automotive Seat

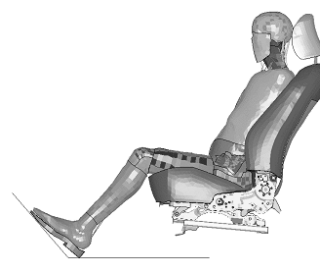
An automotive seat is shown in Figure 9. The seat consists of shell parts such as frame, panel, pipe, fabric and others modeled by shell elements, cushion and backrest spring modeled by beam, and solid urethan placed in the head rest, backrest, and cushion. Each part is modeled precisely, according to its geometry.

### 4.2 Validation of FE model

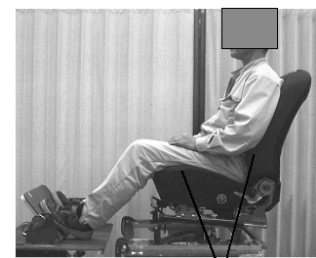
In the FE analysis, the THUMS is seated with gravity on a prototype seat as shown in Figure 10. In the experiment, the same subject as for rigid seat experiments, was seated. Pressure distribution was recorded and the subject was again asked to evaluate whether his hip was sliding or not.



Fig. 9: Automotive Seat Model



(a) Simulation model



Pressure Sensor

(b) Experiment

Fig. 10: Seating Setup

4.2.1 Pressure Distribution

The comparison of seat pressure distribution between the simulation and the experiments is shown in Figure 11. The simulation results are overlaid by a skeleton frame to easily understand the relative location between the pressure and the bony parts. A good correlation was found: 1) High pressure areas were located at the lumbar area and the lower part of the scapula for the backrest., 2) Highest the pressures were found at the ischium tuberosities and thigh areas for the seat.

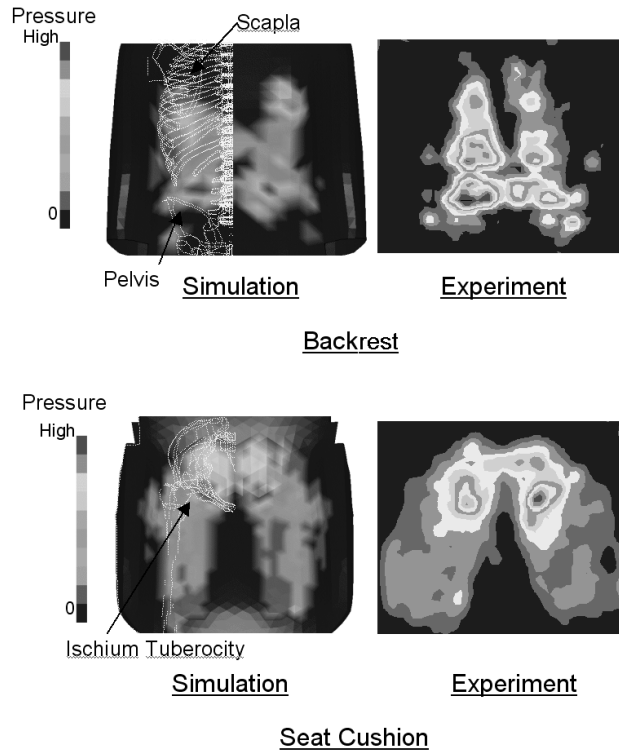


Fig. 11: Comparison of Seat Pressure

The cumulative pressure distribution diagram for the seat cushion is shown in Figure 12. The dotted line with white square markers shows the FE result, and solid line with black square markers shows experimental results.

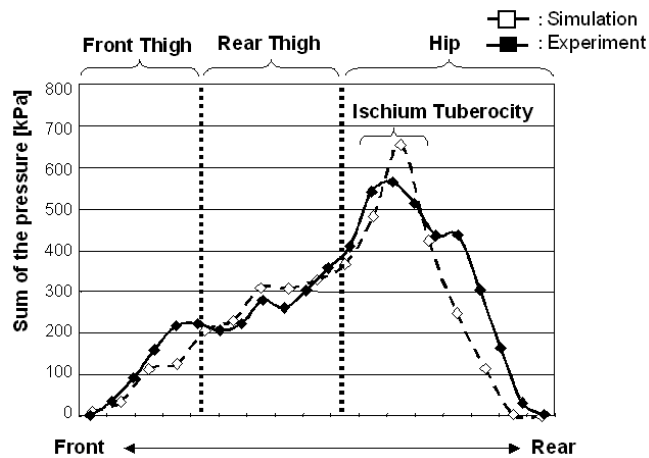


Fig. 12: Balance Diagram of Seat Cushion Pressure

The pressure increases gradually from front end to rear, and becomes maximum at ischium tuberosity. Then the pressure decreases rapidly to the rear end. Comparison between simulation and experiment shows that the maximum pressure at ischium tuberosities of the simulation is higher than that of experiment, and is lower in rear end. It is conjectured that this difference might be caused by differences in flesh volume between THUMS and the tested subject. The importance of hip tuberosity force on hip sliding generation was shown in section 3.2. The possible over estimation of CAE tuberosity pressure might result in higher sliding estimation compared to test on human subjects. That difference is not judged too severe in this case because seat reaction force lever arm with respect to hip center of gravity is small.

#### 4.2.2 Amount of Hip Sliding

The amount of hip sliding evaluated by THUMS is compared with that measured in experiment. In the experiment, the movement of pressure point at ischium tuberosity is defined as amount of hip sliding. The simulation result of the amount of hip sliding 7 mm well coincide with the experimental result 6 mm. The perception of the subject to this seat is "With hip sliding" in the experiment.

#### 4.3 Confirmation of Hip Sliding Equation

In addition to the automotive seat A, the hip sliding performance is estimated for a countermeasured seat B. In the seat B, the cushion spring is softened to increase the hip cushion angle ( $\theta_{Hip}$ ), and the thickness of the cushion front end is increased to reduce the the hip force ( $F_1$ ). The simulated pressure distributions of the seat A and B are shown in Figure 13. It was found that the pressure around the ischium tuberosities decreased in seat B comparing to the seat A. And also that the pressure increased around the front end and cushion side in the seat B.

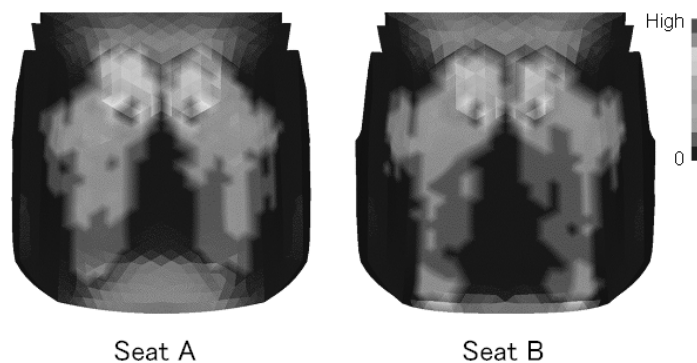


Fig. 13: Simulation Results of Seat Pressure

A cross section shows the deformation of the cushion in Figure 14. The black line is seat A, and the gray line is seat B. It is found that the deformation of the cushion underneath ischium tuberosities increases in seat B comparing to the seat A. The amount of hip sliding which was evaluated as 7 mm in seat A, become 3 mm in the seat B. Hip sliding is small in seat B (ischium tuberosity displacement is below 5 mm). A subject will not detect it. The result of the hip cushion angle ( $\theta_{Hip}$ ) and hip force ( $F_1$ ) of the seat A and B are plotted in Figure 8 together with the hip sliding equation (Figure 15). The black square mark is the result of seat A and the white square mark is that of seat B. The hip forces are 392 N and 375 N, and the hip cushion angles are 10 degree and 15 degree for the seat A and seat B respectively. Consequently, it is expected that the seat A will generate hip sliding but not the seat B. The 100 N difference for hip force in seats A and B and rigid flat seat is due to the fact that forces are more distributed along thighs and backrest.

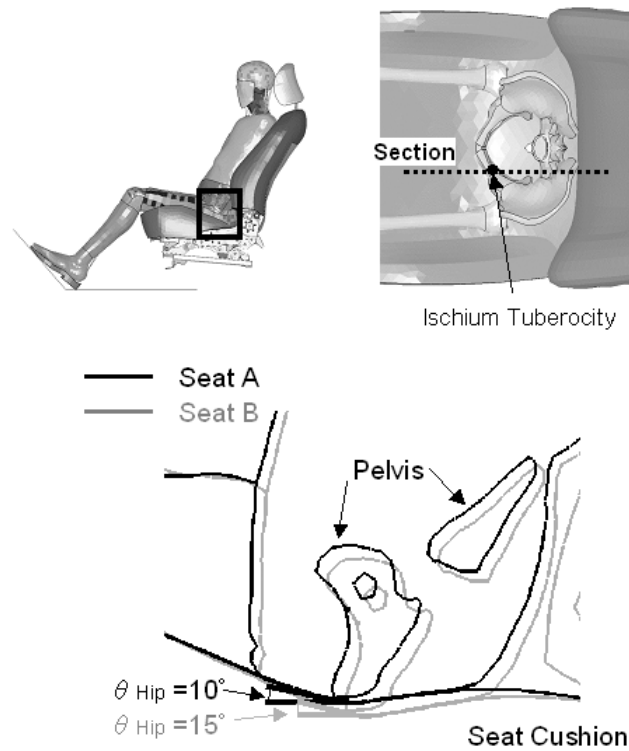


Fig. 14: Comparison of Seat Deformation

Following simulations, experiments using prototypes of seat A and B were conducted, with nine subjects. The result of subjective evaluation is shown in Figure 16. The subjects are seven males (ranging 163-184 cm height, average:171.6 cm) and females (150 and 158 cm height). Test subjects were requested to judge seat hip sliding as "bad:1, 2", "acceptable: 3 to 5" and "good: 6, 7". The seat adjusters such as backrest, rail, cushion height are set for all subjects at middle range. These results show that the seat B obtains good evaluation of hip sliding comparing to the seat A, and that agreed with the estimation of the hip sliding equation derived from THUMS analysis.

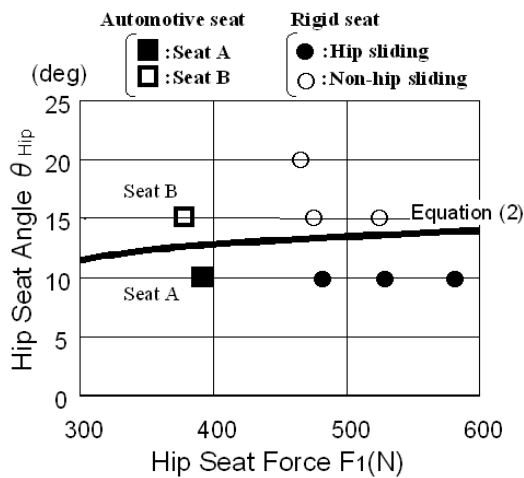


Fig. 15: Automotive seats on the Hip Sliding Condition

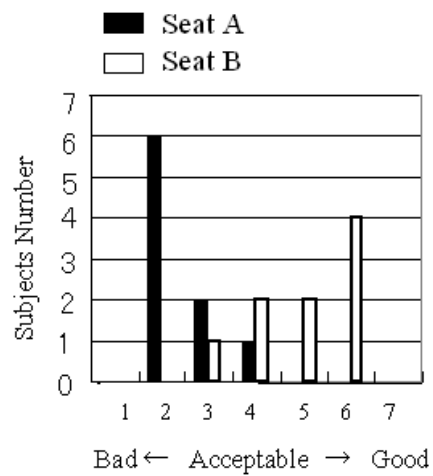


Fig. 16: Results of Hip Sliding Subjective Evaluation

## 5 Conclusions

1. Hip sliding mechanisms was analyzed by quantifying the moment around the hip centre of gravity using a human body FE model.
2. The main factor affecting hip sliding is the hip seat reaction force generated around the ischium tuberosities of the pelvis. Therefore a larger hip seat reaction force or a larger lever arm of this force vector to the hip centre of gravity are likely to increase hip sliding effect.
3. The hip sliding equation was derived from the relationship between the hip force from the seat cushion and the cushion angle underneath the hip.
4. Tests and CAE results in the case of automotive seats have good agreement and confirm the equation obtained from analytical study.

The authors would like to thank staff members who took an active part in the experiments.

## 6 References

- [1] Matsuoka, M., Niwano, A., Morita, A.: "Design of Swing-seat Function Using Simulation of Hip-sliding Force", BULLETIN OF JSSD, Vol.47, No.5, 2001, pp.65-72
- [2] Su-Hwan Hwang, et al.: "Digital and Physical Human Body Models for Seat Comfort Evaluation", JSAE 20085057
- [3] Rasmussen, J., Zee, M., Torholm, S.: "Muscle Relaxation and Shear Force Reduction May Be Conflicting: A Computational Model of Seating", SAE 2007-01-2456
- [4] Yamada, H.: "Strength of Biological Materials", F.G.Evans, editor, The Williams & Wilkins Company, Baltimore, 1970
- [5] Kohara, J., Sugi, T.: "Development of Biomechanical Manikins for Measuring Seat Comfort", SAE 720006